

REVIEW ARTICLE

Optical and non-optical methods for detection and characterization of microparticles and exosomes

E. VAN DER POL,*† A. G. HOEKSTRA,‡ A. STURK,* C. OTTO,§ T. G. VAN LEEUWEN,†¶ and R. NIEUWLAND*

*Laboratory of Experimental Clinical Chemistry and †Biomedical Engineering and Physics, Academic Medical Center, University of Amsterdam, Amsterdam; ‡Computational Science, Faculty of Science, University of Amsterdam, Amsterdam; §Medical Cell BioPhysics, University of Twente, Enschede; and ¶Biomedical Photonic Imaging, University of Twente, Enschede, the Netherlands

To cite this article: van der Pol E, Hoekstra AG, Sturk A, Otto C, van Leeuwen TG, Nieuwland R. Optical and non-optical methods for detection and characterization of microparticles and exosomes. *J Thromb Haemost* 2010; **8**: 2596–607.

Summary. Microparticles and exosomes are cell-derived microvesicles present in body fluids that play a role in coagulation, inflammation, cellular homeostasis and survival, intercellular communication, and transport. Despite increasing scientific and clinical interest, no standard procedures are available for the isolation, detection and characterization of microparticles and exosomes, because their size is below the reach of conventional detection methods. Our objective is to give an overview of currently available and potentially applicable methods for optical and non-optical determination of the size, concentration, morphology, biochemical composition and cellular origin of microparticles and exosomes. The working principle of all methods is briefly discussed, as well as their applications and limitations based on the underlying physical parameters of the technique. For most methods, the expected size distribution for a given microvesicle population is determined. The explanations of the physical background and the outcomes of our calculations provide insights into the capabilities of each method and make a comparison possible between the discussed methods. In conclusion, several (combinations of) methods can detect clinically relevant properties of microparticles and exosomes. These methods should be further explored and validated by comparing measurement results so that accurate, reliable and fast solutions come within reach.

Keywords: characterization, exosomes, microparticles, microvesicles, optical detection.

Introduction

Cells release microvesicles that function as vehicles for the transport and delivery of cargo between cells [1,2]. In addition, microvesicles promote coagulation and inflammation. Throughout this article, we will use ‘microvesicles’ as a generic term for all types of cell-derived extracellular vesicle, unless stated otherwise. Although the clinical interest and relevance of microvesicles is increasingly recognized [3], their isolation and detection is still cumbersome [4]. At present, novel detection methods are being explored [5–9]. This article is an assessment of the accuracy and practicability of methods for the detection of microvesicles.

Microparticles and exosomes

The best studied types of microvesicle are exosomes and microparticles. Although a generally accepted definition is lacking [10,11], there are several features characterizing exosomes and microparticles. Exosomes are released from cells containing multivesicular bodies when the membranes of multivesicular bodies fuse with the plasma membrane. By transmission electron microscopy (TEM), exosomes appear with characteristic doughnut morphology, and their diameter ranges between 30 and 100 nm [12]. Their density ranges from 1.13 to 1.19 g mL⁻¹ [13], and proteomes contain characteristic but not unique protein families, including heat shock proteins and tetraspannins [14]. The main function of exosomes is to modulate the immune response [15].

Microparticles are released from the plasma membrane during ‘budding’ or ‘shedding’. Most, if not all, eukaryotic cells release microparticles, especially during conditions related to stress, such as activation and apoptosis [16]. Microparticles are larger and more heterogeneous in morphology than exosomes, with reported diameters ranging between 100 nm and 1 μm [17]. Microparticles are best known for binding coagulation factors and exposing tissue factor [18–20]. Their absence is associated with a bleeding tendency [21], and their (increased) presence is associated with disseminated intravascular coagulation and

Correspondence: E. van der Pol, Academic Medical Center, University of Amsterdam, Biomedical Engineering and Physics, Meibergdreef 9, 1105 AZ Amsterdam, the Netherlands.

Tel.: +31 20 5664386; fax +31 20 6917233.

E-mail: e.vanderpol@amc.uva.nl

Received 24 February 2010, accepted 6 September 2010

thrombosis [22,23]. There is increasing evidence that exosomes and microparticles are 'multipurpose carriers' facilitating the intercellular exchange of transmembrane receptors, mRNA, microRNA, and signaling molecules [24–26]. Furthermore, they promote cellular survival by removing dangerous or redundant intracellular compounds [27–29].

Microvesicle isolation, detection, and characterization

Currently, progress in microvesicle research is hampered by several factors. Because of the biological complexity of body fluids, isolation of microvesicles has proven to be extremely difficult. For instance, isolation of microvesicles from blood is affected by venepuncture, time between blood collection and handling, the anticoagulant, centrifugation and washing procedures, the presence of lipoprotein particles and small platelets within the size range of microvesicles, the high viscosity of blood, and the presence of sticky proteins, including fibrinogen and albumin. Because of their small size, microvesicles are below the detection range of conventional detection methods. As a consequence, recovery and contamination cannot be reliably quantified, and isolation protocols have not been standardized. For example, conflicting results were reported on the procoagulant properties of microvesicles from sickle cell disease patients [30,31]. Both studies attributed the procoagulant features to 'microparticles', but they used markedly different isolation protocols, involving centrifugation at $18\,890 \times g$ [30] or $100\,000 \times g$ [31], presumed to result in isolation of microparticles or microparticles and exosomes, respectively.

Clinically relevant properties of microvesicles

In this review, currently available and potentially applicable methods for the detection and characterization of microvesicles are presented. Clinically relevant properties of microvesicles are size, concentration, morphology, biochemical composition, and cellular origin. From the size information of individual microvesicles, a relative size distribution can be obtained, providing insights into the number of microvesicles of one particular size relative to those of another size. We define concentration as the number of microvesicles per unit volume. If both the relative size distribution and concentration are known, an absolute size distribution can be obtained, which gives the number of microvesicles of one particular size per unit volume. By morphology, we mean shape and ultrastructure. Ultrastructure is illustrated in Fig. 1A, where microvesicles differ not only in shape but also in contrast and surface pattern. The biochemical composition refers to the biological and chemical components of which microvesicles are composed. The cellular origin refers to the cell type from which the microvesicles originate.

Standard population and outline

For each detection method, the working principle is briefly explained and the measurement time is estimated, assuming the

detection of 10 000 particles, a number that is common in flow cytometry. In addition, we give a prediction of the performance of each method in detecting size, concentration, morphology, biochemical composition, and cellular origin, by considering the underlying physical parameters of the methods. To compare the performance of the methods for size detection, we made a model predicting the size distribution for a given population of microvesicles. As outlined previously, isolation of microvesicles from blood is a challenge. Therefore, we arbitrarily chose microvesicles from urine to create a standard population as a realistic input for our model. Urine can be used to prepare a relatively high concentration of microvesicles without excessive contamination with, for example, platelets or proteins.

To create the standard population, we isolated microvesicles from fresh cell-free urine of a healthy male individual by high-speed centrifugation (Fig. 1A; 30 min at $18\,900 \times g$), followed by ultracentrifugation of the supernatant (Fig. 1B; 1 h at $154\,000 \times g$). We imaged microvesicles by TEM and measured the diameter of 500 microvesicles in each fraction. The combined size distributions are shown in Fig. 1C. As different size distributions of microvesicles in blood have been reported [5,6,32,33], it is difficult to compare our standard population with its plasma counterpart. Nevertheless, our standard population corresponds well with recent data on the size distribution of plasma microvesicles [5]. One has to bear in mind that the reported absolute size distributions are affected by isolation procedures. In the literature, microvesicle concentrations in plasma range from 10^7 to 10^{12} L^{-1} [5,9,33–36]. As our simulations demand an absolute size distribution as input, we arbitrarily multiplied our relative microvesicle size distribution by 10^9 L^{-1} , as this concentration is usually reported in plasma.

The outline of this review is as follows. The first part describes optical detection, and is subdivided into methods based on light scattering or fluorescence. The second part describes non-optical detection methods. Table 1 provides an overview of all detection methods.

Optical methods

Optical methods have the potential to accurately obtain all clinically relevant properties of single microvesicles at a high speed. Two important parameters in optics are the wavelength of light and the refractive index of particles relative to the suspending medium. Optical phenomena, including reflection and refraction, depend on the refractive index n of the material. The refractive index depends on the wavelength λ , and is defined as the ratio of the speed of light in vacuum to that in the material. In practice, the higher the difference between the refractive index of a microvesicle and its surroundings, the more light will be scattered.

Light scattering

Light that illuminates a microvesicle is partly absorbed and partly scattered. As many optical setups are based on the

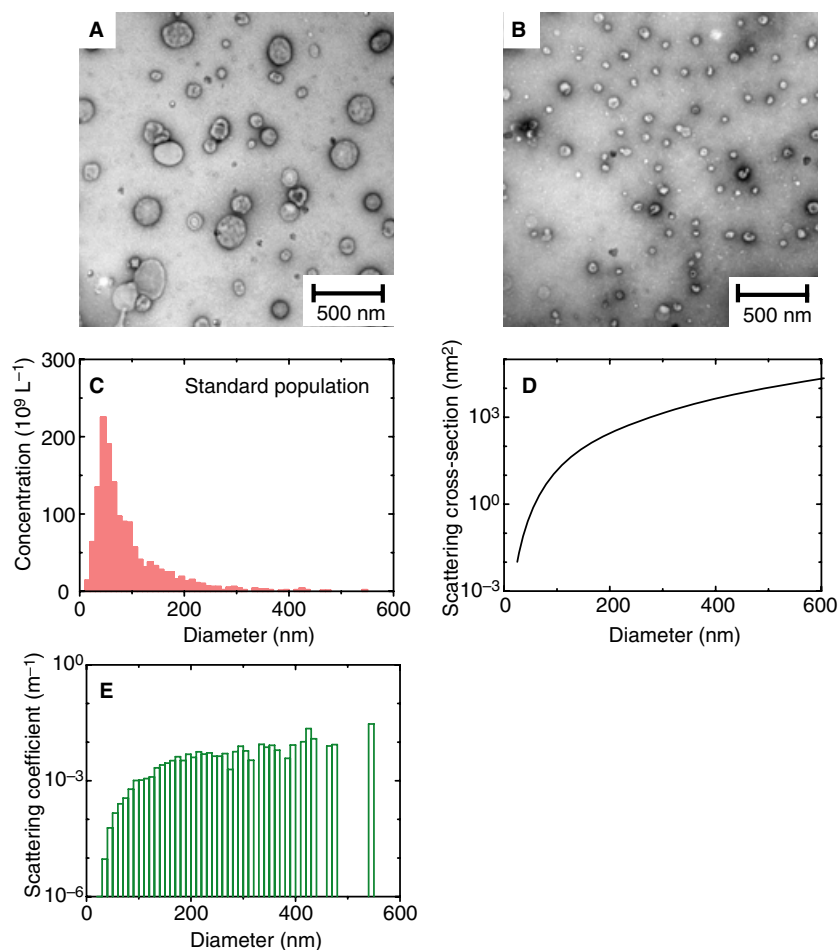


Fig. 1. Transmission electron microscopy (TEM) of microvesicles from fresh cell-free human urine. (A) Microvesicles isolated from cell-free human urine by centrifugation (30 min at $18\,900 \times g$). (B) Microvesicles isolated from microparticle-depleted urine by ultracentrifugation (1 h at $154\,000 \times g$). (C) Concentration vs. diameter for microvesicles as measured by TEM, and referred to as the standard population. The plot shows a broad distribution between 20 and 440 nm, with a single peak at 45 nm. (D) Scattering cross-section vs. diameter (logarithmic scale) for microvesicles, calculated using Mie theory of a sphere ($n_p = 1.38$) surrounded by a membrane (10 nm; $n_s = 1.48$). The medium is water ($n_m = 1.33$) and the wavelength of the laser is 532 nm. The scattering cross-section, and thus the quantity of light scattered by a microvesicle, strongly decreases with decreasing diameter. (E) Scattering coefficient vs. diameter (logarithmic scale) for the standard population. The scattering coefficient, which is the average number of scattering events that light encounters per unit length, is given by the product of the concentration of the standard population and the scattering cross-section. The scattering coefficient strongly increases with increasing diameter, indicating that the contribution of light scattered by microvesicles smaller than 100 nm is relatively small.

detection of scattered light, it is important to know how much light is scattered by a single microvesicle. The quantity of light scattered by a single microvesicle is proportional to the scattering cross-section σ . When the diameter is at least 10 times smaller than the wavelength, the Rayleigh approximation can be applied to calculate the scattering cross-section,

$$\sigma \propto \frac{d^6}{\lambda^4} \left(\frac{m^2 - 1}{m^2 + 2} \right)^2 \quad (1)$$

where \propto denotes 'proportional to', d is the particle diameter, and $m = n_v/n_m$ is the refractive index ratio of the vesicle and the medium [37]. At a wavelength of 532 nm, which is commonly used in optical devices, the Rayleigh approximation can be applied to particles of $532/10 \approx 50$ nm and smaller, which is typically the size of the smallest exosomes.

From Eqn 1, it follows that if a microvesicle is only 10-fold smaller than another microvesicle, the scattering cross-section and thus the scattered amount of light decreases 10^6 -fold.

Mie theory provides exact predictions of the absorption and scattering of light from spheres with arbitrary diameter and refractive index [38]. The solid line in Fig. 1D shows the scattering cross-section vs. the diameter for a sphere that contains a high refractive index shell, for example a phospholipid membrane, as calculated with Mie theory. The calculation parameters are chosen to be as realistic as possible for the case of microvesicles. Fig. 1D, in a semi-logarithmic representation, shows that the scattering cross-section drops rapidly for smaller microvesicles. To illustrate how this decrease affects light scattered from all microvesicles of the standard population, the concentration (Fig. 1C) is multiplied by the scattering

Table 1 Assessed capabilities of (potential) methods for the detection of microvesicles, based on the underlying physical parameters of the method

Method	Resolution (nm)	Detection limit	Size distribution	Requirements and/or assumptions	Concentration	Requirements and/or assumptions	Biochemical information	Measurement time
Optical methods								
Scattering								
Optical microscopy	200	≥ 10 nm	-		+/-	V_d	-	H
Scattering flow cytometry		≥ 300 nm	-	Calibration with beads	+/-	Q	+/-	S
DLS		1 nm to 6 μm	+/-	$T, \eta, n_s, n_s, \text{model}$	-		-	M
NTA	1000	50 nm to 1 μm	+/-	T, η	+/-	Calibration with beads	-	M
Raman spectroscopy	350	To be investigated	?	Raman signal $\propto d$	+/-	V_d	+	H
Fluorescence								
Fluorescence microscopy	200	Single molecule/QD	-	Fluorescence signal $\propto d$	+/-	V_d	+	H
STED microscopy	30	Single molecule/QD	+	Surface labeling	+/-	V_d	+	H
Fluorescence flow cytometry		Single QD	-	Fluorescence signal $\propto d$	+/-	Q	+	S
Fluorescence correlation spectroscopy		Single molecule/QD	+/-	$T, \eta, V_d, \text{model}$	+	V_d	+	M
F-NTA	600	Single QD	+	T, η	+	Calibration with beads	+	M
Non-optical methods								
TEM	~ 1	< 1 nm	+	No shrinkage	-		+/-	H
AFM	< 1	≥ 300 nm	+	Isovolometric deformation	+/-	100% surface binding	+	H
Impedance-based flow cytometry			-	d_c, l_c	+/-	$d_c, v_{s,av}$	-	S

AFM, atomic force microscopy; DLS, dynamic light scattering; F-NTA, fluorescence nanoparticle tracking analysis; NTA, nanoparticle tracking analysis; QD, Quantum Dot; STED, stimulated emission depletion; TEM, transmission electron microscopy. For each method, the resolution, detection limit, ability to measure the size distribution and concentration, ability to provide biochemical information, and the measurement time are estimated. Requirements of the method and/or assumptions that have to be made to determine the size distribution and concentration are also listed. d is the microvesicle diameter, d_c is the channel diameter, l_c is the channel length, η is the viscosity of the solvent, n_s is the refractive index of the particle, n_s is the refractive index of the solvent, Q is the flow rate, T is the temperature of the solvent, V_d is the detection volume, and $v_{s,av}$ is the average particle transport velocity. A method that is incapable, capable but with limitations, or capable of providing information on the size distribution, particle concentration or biochemical composition is indicated by -, +/-, and +, respectively. The measurement time is indicated by S, M, and H, which mean shorter than 1 min, between 1 min and 1 h, and longer than 1 h, respectively.

cross-section (Fig. 1D) to obtain the scattering coefficient per diameter (Fig. 1E). The scattering coefficient, depicting the mean number of scattering events of the light per unit length, is a measure of the amount of light scattered by all microvesicles per diameter. Please note that the contribution of light scattered by microvesicles smaller than 100 nm is surprisingly small (Fig. 1E), given their high concentration (Fig. 1C). Consequently, smaller microvesicles require more sensitive optical detection than larger microvesicles, and scattering of small particles can easily be overwhelmed by scattering of large particles.

Optical microscopy In a bright-field optical microscope, the sample is illuminated by visible light. Scattered light from the sample is collected by a microscope objective and focused on a charge-coupled device (CCD) camera. The resolution is the shortest distance between two adjacent points that can be distinguished by an optical microscope. The best achievable resolution R is given by the Rayleigh criterion,

$$R = \frac{1.22\lambda}{2NA} \quad (2)$$

where NA is the numerical aperture of the microscope objective. NA characterizes the range of angles over which the microscope objective accepts light. Oil-immersion microscope objectives have an NA up to 1.4. Assuming a wavelength of 532 nm, the best resolution of a standard optical microscope is approximately 200 nm. So, it is impossible to measure the size and morphology of microvesicles smaller than 200 nm by optical imaging. Despite this limitation, gold particles down to 10 nm in diameter have been detected, because gold particles scatter light very efficiently [39]. They appear as bright spots, but their true particle size is hard to determine. For microvesicles with light scattering higher than the detection limit, an estimation of the concentration can be made from the count of the number of scatter events if the detection volume V_d is known. The time needed to measure 10 000 microvesicles with a standard optical microscope is in the order of hours, and no information on the biochemical composition or cellular origin is provided.

Scattering flow cytometry Flow cytometry is well known for counting and separating single cells (diameter > 1 μm) in fluids at a rate of thousands per second. Most flow cytometers can detect scattered light and fluorescence. In this section, we consider only light scattering.

A flow cytometer guides cells and microvesicles through a laser beam in a hydrodynamically focused fluid stream. One detector is placed in line with the laser beam and measures the forward scattered light (FSC). A second detector measures the side scattered light (SSC) perpendicular to the beam. From light-scattering theory, the following approximate results can be expected. Particles larger than the wavelength of light, such as cells, predominantly scatter light in a forward direction. Hence, FSC is associated with particle size. Particles smaller than the wavelength, such as organelles, scatter relatively more

light in a perpendicular direction, so SSC is associated with the complex anatomy of cells. In reality, however, light scattering is a complex process. Therefore, light scattering of biological particles is an active research field [40,41].

A flow cytometer performs well in the distinction of cell types, but has major drawbacks in determining the size of microvesicles. First, the lower detection limit of commercial flow cytometers for polystyrene beads is 300–500 nm [8,33,42]. Consequently, only a small fraction of microvesicles can be detected. Second, only particles that differ by approximately 280 nm or more in size can be resolved with flow cytometers [8,33]. Third, quantitative size information is obtained by comparing the scattering intensity of microvesicles with that of beads of known size. The scattering intensity, however, depends not only on size but also on shape, refractive index, and absorption. The refractive index and absorption are even interconnected via Kramers–Kronig relationships [43]. For example, according to Mie calculations, a spherical gold particle 200 nm in diameter scatters 27 times more light than a polystyrene sphere of a similar size, which, in turn, scatters 15 times more light than a microvesicle, owing to refractive index differences. Furthermore, for non-spherical geometries, complex computer simulations are required [44].

Figure 2A shows an impression of the size distribution as calculated for a flow cytometer in scattering mode, using the standard population as input. As the detection limit is approximately 300 nm, smaller microvesicles are detected with low efficiency [8,33]. Consequently, the measurements do not reflect the standard population. The poor capability to resolve size differences results in a smooth curve. The concentration of microvesicles can be estimated when the flow rate Q is known. No specific information on morphology is obtained from the light-scattering intensity.

Biochemical information is obtained by correlating the FSC with the SSC signal. As microvesicles have a size in the order of the wavelength of visible light or smaller, they scatter light substantially in a perpendicular direction. Side scatter from a large microvesicle therefore overwhelms side scatter from smaller structures inside. As a consequence, distinguishing microvesicles with different cellular origins by correlating FSC and SSC signals is difficult, but it can be improved by analyzing the polarization of sideward scattered light [45].

Dynamic light scattering (DLS) DLS, also known as photon correlation spectroscopy or quasi-elastic light scattering, determines the relative size distribution in a fluid of particles ranging in size between 1 nm and 6 μm [46,47]. Particles in a fluid continuously move in random directions, owing to continuous collisions with solvent molecules. This causes a random motion of particles called Brownian motion. The velocity distribution of particles depends on the temperature T , viscosity η , and (hydrodynamic) particle diameter d . The smaller the particle, the faster the Brownian motion. Particles undergoing Brownian motion cause intensity fluctuations of scattered light, which is measured typically in 30 s. The relative size distribution is obtained from the intensity

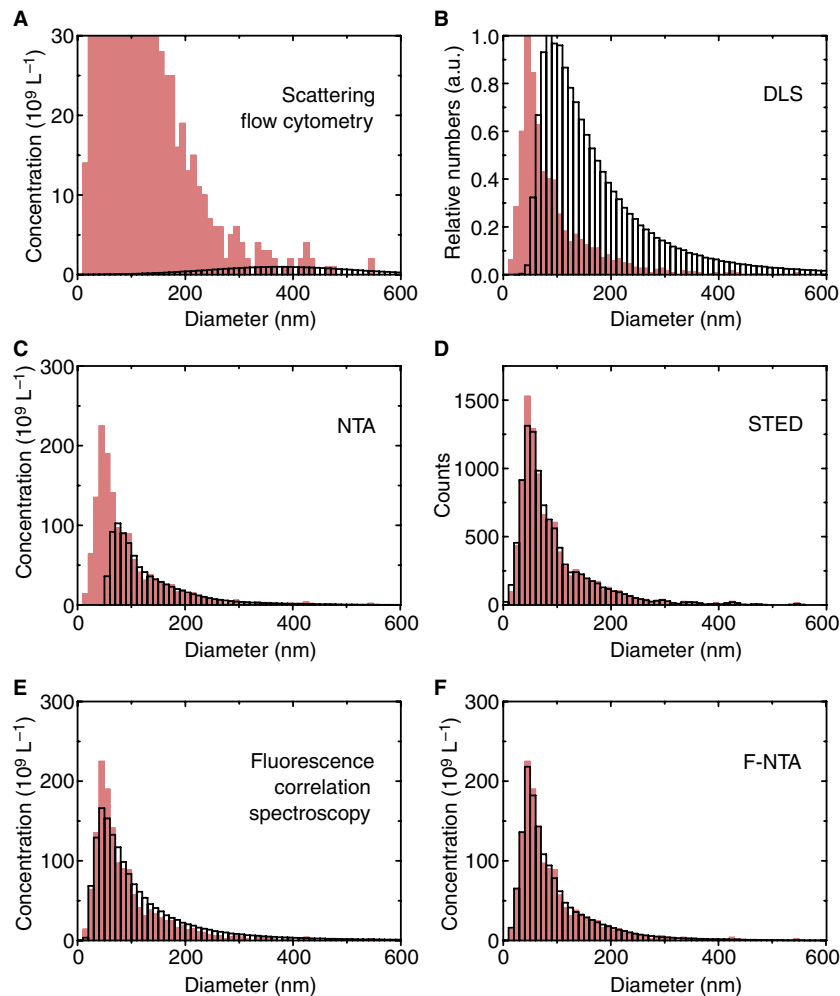


Fig. 2. Calculated size distribution for optical detection methods (open black) relative to the standard population (transparent red), based on the underlying physical parameters of each method. (A) Scattering flow cytometry determines concentration vs. diameter. Microvesicles larger than 300 nm in diameter are detected, but microvesicles smaller than 300 nm are detected with low efficiency. (B) Dynamic light scattering (DLS) determines the relative size distribution. The distribution is normalized to 1, and shows a shift to larger diameters. (C) Nanoparticle tracking analysis (NTA) determines the absolute size distribution with high precision for microvesicles larger than 100 nm, but is currently not sensitive enough to detect microvesicles smaller than 50 nm. (D) Stimulated emission depletion (STED) microscopy determines counts vs. diameter. The distribution is normalized to a total count of 10 000 microvesicles, and shows a high correlation with the standard population. (E, F) Both fluorescence correlation spectroscopy (E) and fluorescence NTA (F-NTA) (F) determine the absolute size distribution, which shows a high correlation with the standard population. The Pearson correlation coefficients between the calculated distribution and the standard population are -0.61 (scattering flow cytometry), 0.40 (DLS), 0.53 (NTA), 1.00 (STED), 0.98 (fluorescence correlation spectroscopy), and 1.00 (F-NTA).

fluctuations by applying a mathematical algorithm following from light-scattering theory. Light scattering theory requires the refractive index difference $n_v - n_s$ between the solvent and microvesicles, which is currently unknown. DLS performs well in the size determination of monodisperse samples, i.e. samples containing particles of one particular size, and monitoring a change in a sample such as aggregation [48–50]. Detection of the size distribution of polydisperse samples, i.e. samples containing different-sized particles, is less accurate, as the measured size distribution is highly influenced by the presence of small numbers of larger particles, such as platelets or other contaminants, which scatter more light than small vesicles, as shown in Fig. 1D [49,50]. Furthermore, the result strongly

depends on the applied mathematical algorithm [48,49], and two populations can only be resolved if the particle diameter differs at least two-fold [48–51].

Figure 2B shows the calculated relative size distribution for DLS relative to the standard population. The maximum value of the distribution is arbitrarily set to 1, as the concentration is unknown. Because larger microvesicles scatter light more efficiently than smaller ones, the smallest microvesicles become undetectable, and the distribution shifts to larger diameters. Our calculations closely fit the size distribution measurement of microvesicles from fresh frozen plasma obtained with the N5 Submicron Particle Size Analyzer [6]. DLS does not provide information on the biochemical composition or cellular origin.

Nanoparticle tracking analysis (NTA) NTA measures the absolute size distribution of particles ranging in size from 50 nm for biological particles to 1 μm . Particles in a fluid are illuminated by a laser beam and therefore scatter light, which is collected by a conventional optical microscope. NTA visualizes the scattered light from single particles in the field of view of the microscope. The scattered light shows up as small bright spots moving because of Brownian motion. The movements of individual particles are followed through a video sequence acquired over one to several minutes, and the mean velocity of each particle is calculated with image analysis software [36]. Because the velocity of Brownian motion depends on the temperature T , viscosity η , and (hydrodynamic) particle diameter d , it is possible to obtain an absolute size distribution after system calibration with beads of known size and concentration.

Figure 2C shows the calculated absolute size distribution for NTA. On the basis of our assessment, NTA performs well for microvesicles larger than 50 nm, but detection of microvesicles smaller than 50 nm is not possible, owing to the detection limit of the microscope. NTA does not detect biochemical composition or cellular origin.

Raman spectroscopy Raman spectroscopy is an inelastic light-scattering technique used to reveal the structure and biochemical composition of macromolecules inside single living cells [52,53]. The sample is illuminated by monochromatic laser light. Molecular vibrations in the sample cause an energy loss or gain during a scattering event, resulting in a change in wavelength of the scattered light, which can be detected by specialized, sensitive spectrometers. The pattern of molecular vibrations is molecule-specific. As microvesicles are composed of many different biomolecules, which all have unique Raman spectra, the chemical composition can be investigated without labeling. A confocal Raman microspectrometer can detect the Raman spectrum of volume elements of approximately $0.3 \mu\text{m}^3$ [54,55], which overlaps with the dimension of microvesicles, such that the chemical composition of single microvesicles can potentially be detected without labeling. Furthermore, Raman microspectroscopy is a quantitative technique. The signal strength is linearly proportional to the number of molecules. For a microvesicle that fits within the probe volume, the magnitude of the Raman signal strength is proportional to the volume of a single microvesicle, and therefore estimates the relative size; this is a method that warrants further investigation before a reliable comparison with the standard population can be made. The concentration can be determined if the detection volume V_d is known. The estimated measurement time is 3 h.

Fluorescence

Fluorescence is the property of a material whereby it absorbs light of a particular wavelength and re-emits it at a usually longer wavelength. Most cells and microvesicles exhibit no intrinsic fluorescence by which they can be distinguished.

Therefore, microvesicles are labeled with conjugates of antibodies or proteins with fluorophores [56]. Commonly used fluorophores are organic dye molecules and quantum dots. Quantum dots have a typical diameter of 2–20 nm, and have been used as an artificial light source with which a microvesicle can be labeled [57]. In general, quantum dots are brighter and more stable than organic dye molecules or fluorescent proteins. As microvesicles usually expose antigens from the parental cells, all methods based on fluorescence detection potentially provide information on the biochemical composition and cellular origin of microvesicles. Fluorescence also offers opportunities to acquire additional chemical information, as the fluorescence intensity, wavelength and average time for which light is absorbed (fluorescence lifetime) depend on the molecular environment [58,59].

Fluorescent multilabeling analysis is not easy to perform, and there are several practical problems. For example, antibodies usually bind not only to the antigen of interest but also to Fc receptors. Furthermore, antibodies adhere non-specifically or form aggregates, interfering with quantitative optical methods [60]. In addition, other optical difficulties limit the feasibility of fluorescence detection. For example, it may be difficult to distinguish the fluorescence signal of interest from background radiation caused by autofluorescence, or irreversible photobleaching of fluorophores may occur [61]. In the case of multilabeling, fluorophores can spectrally overlap, such that fluorescence associated with one fluorophore is detected by more than one detector [62].

Fluorescence microscopy A fluorescence microscope is an optical microscope optimized for fluorescence detection. Usually, the fluorescence emission is separated from the excitation light with a spectral filter, before detection by a CCD camera. Modern fluorescence microscopes are able to detect fluorescence from a single fluorophore. For example, Zhang *et al.* [57] loaded a synaptic vesicle with a single quantum dot (approximately 15 nm) to monitor membrane fusion and retrieval by high-speed imaging fluorescence microscopy.

In the case of autofluorescence, the size of microvesicles can conceptually be determined, as the fluorescence signal may be proportional to the microvesicle volume. However, in the case of fluorescent labeling, it is highly unlikely that the fluorescent amplitude will be proportional to the volume, so no size information can be obtained. Fluorescence microscopy allows an assessment of the concentration of microvesicles with a certain property under the assumption that all microvesicles with that property are indeed labeled and that the detection volume V_d is known. A typical measurement time is approximately 1 h.

Stimulated emission depletion (STED) microscopy In practice, STED microscopy is high-resolution fluorescence microscopy with better spatial resolution than described by Eqn 2 for diffraction-limited optics. A resolution of 16 nm in diameter was successfully demonstrated, and this is sufficiently small to size microvesicles [63,64]. Figure 2D shows the

calculated size distribution. The predicted distribution correlates well with the standard population. Not only is STED microscopy promising for determining the size of and locating fluorescently labeled microvesicles, but the high resolution can potentially be used to gain information on morphology and to determine the distribution of labeled receptors at the surface of larger microvesicles, just as is presently done for organelles inside living cells [65]. The concentration can be determined if the detection volume V_d is known, and the measurement time for probing 10 000 particles is in the order of hours.

Fluorescence flow cytometry In a fluorescence flow cytometer, the fluorescence from single particles present in a hydrodynamically focused fluid stream is measured at a rate of thousands of particles per second. With fluorescence activated cell sorting, it is possible to distinguish microvesicles on the basis of the spectral properties of the fluorescence signal [8]. For nanometer-sized particles, the fluorescence intensity is higher than the light-scattering intensity, so fluorescence flow cytometry is more sensitive than scattering flow cytometry. Flow cytometers with confocal optics can detect single fluorophores with an efficiency of approximately 10% by minimizing background fluorescence [66]. As in fluorescence microscopy, the size distribution can, in principle, be determined when the amplitude of the fluorescence signal is proportional to the microvesicle volume, a method that warrants further investigation. Fluorescence flow cytometry can estimate the concentration if the flow rate Q is known, again under the assumptions that all microvesicles are labeled and have a fluorescence intensity above the detection limit and threshold of the flow cytometer.

Fluorescence correlation spectroscopy Fluorescence correlation spectroscopy was originally introduced to measure parameters of molecular diffusion [67]. It can determine the absolute size distribution and fluorescence signal of particles in a fluid [68]. The size distribution is obtained from fluorescence intensity fluctuations caused by particles moving by Brownian motion through a well-characterized illuminated volume. Unlike DLS, fluorescence correlation spectroscopy detects single fluorescent molecules, and is therefore more sensitive for microvesicles smaller than 50 nm; the size distribution can be more accurately determined in the presence of larger microvesicles, and the concentration can be measured if the detection volume V_d is known [68].

Figure 2E shows the calculated absolute size distribution, under the assumption that all microvesicles are labeled. Although good correlation with the standard population can be simulated, we should be aware that small numbers of larger particles may influence the size distribution substantially. The measurement time is in the order of minutes.

Fluorescence NTA (F-NTA) Fluorescence NTA (F-NTA) determines the absolute size distribution and fluorescence signal of particles in a fluid. The method is

similar to NTA, but is based on tracking of fluorescent particles. F-NTA is an extremely sensitive method for microvesicles in the size range of exosomes, because the fluorescence intensity is considerably higher than the light-scattering intensity. With F-NTA, individual quantum dots can also be detected. The good size and concentration detection properties are illustrated in Fig. 2F. Here, the simulations of the absolute size distribution of microvesicles by F-NTA show an excellent correlation with the standard population.

Non-optical methods

TEM TEM uses electrons instead of photons to create an image. The best achievable imaging resolution of TEM is given by Eqn 2, and depends largely on the spatial stability of the electron beam in combination with the chemical stability of the sample. As the wavelength of electrons is more than three orders of magnitude shorter than the wavelength of visible light, the resolution of TEM can be lower than 1 nm. Because of this high resolution, it is possible to determine the size and morphology of microvesicles [69].

As TEM is performed in a vacuum, biomaterials require fixation and dehydration, which affect size and morphology. Furthermore, the concentration of microvesicles has to be increased by (ultra)centrifugation. As a consequence, the size distribution depends upon preanalytical conditions, and the concentration of microvesicles cannot be determined. With immuno-gold labeling, it is possible to provide biochemical information [69]. The measurement time is in the order of hours.

Atomic force microscopy (AFM) AFM was developed in 1986 by Binnig *et al.* [70], and provides subnanometer-resolution topography imaging. An atomic force microscope consists of a cantilever with a sharp tip at its end that scans a sample surface without physical contact. Movements of the tip are measured, and a three-dimensional image is created by software.

Owing to a lateral resolution of 3 nm and a vertical resolution < 0.1 nm [70], AFM is suitable for size detection and performs better than DLS on polydisperse samples [50]. Siedlecki *et al.* and Yuana *et al.* showed that AFM can be used to measure the relative size distribution of microvesicles in their physiologic state [5,32]. Because of the high resolution of AFM, microvesicles must be bound to an extremely flat surface, such as mica. Antibodies can be used to bind microvesicles to the surface, so that biochemical information can also be obtained [5]. Because the efficiency of microvesicle binding to a surface using antibodies is unknown, the concentration of microvesicles cannot be determined with certainty. Furthermore, the surface binding may affect the morphology of microvesicles, and this may hamper the determination of the real diameter.

Figure 3A shows the calculated relative size distribution for 10 000 counts as measured with AFM, assuming isovolumetric particle deformation and equal surface binding. Under these assumptions, there is excellent correlation with the standard

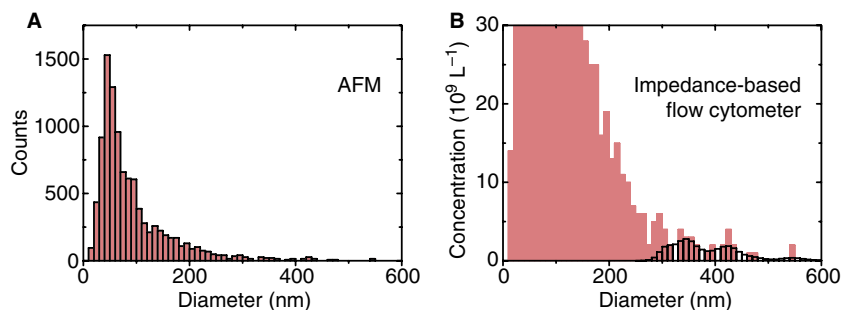


Fig. 3. Calculated size distribution for non-optical detection methods (open black) relative to the standard population (transparent red), based on the underlying physical parameters of each method. (A) Atomic force microscopy (AFM) determines counts vs. diameter. The method can resolve size differences in the order of a few nanometers, and the results show a high correlation with the standard population. (B) Absolute size distribution of a commercial impedance-based flow cytometer with a channel diameter of 25 μm . Microvesicles smaller than 300 nm are detected with low efficiency. The Pearson correlation coefficients between the calculated distribution and the standard population are 1.00 (AFM) and -0.27 (impedance-based flow cytometer).

population, owing to the high resolution. The measurement time is in the order of hours.

Impedance-based flow cytometry The Coulter principle is employed in an impedance-based flow cytometer to count and measure the size of single particles in a fluid within seconds. An impedance-based flow cytometer consists of two chambers divided by an insulating membrane containing a single channel. In each chamber, an electrode is immersed in an electrolyte to drive an ionic current through the channel. Particles driven into the channel cause a reduction in current. A relative size distribution can be calculated from the change in current when the channel length l_c and diameter d_c are known. The concentration can also be determined if the average particle transport velocity $v_{s,av}$ is known.

The sensitivity of impedance-based flow cytometry depends on the channel size with respect to the microvesicle size. The microvesicle diameter must be between approximately 0.1 and 0.7 times the channel diameter [71]. In practice, at least two impedance-based flow cytometers, each with a different channel diameter, are required to cover the whole size range of microvesicles. The lower detection limit of commercial impedance-based flow cytometers is currently 300 nm [9]. Consequently, only a small fraction of microvesicles can be detected.

Figure 3B shows the calculated absolute size distribution for a commercial impedance-based flow cytometer with a channel diameter of 25 μm [9]. As the detection limit is approximately 300 nm, smaller microvesicles are detected with low efficiency. An impedance-based flow cytometer does not provide information on the morphology, biochemical composition, or cellular origin, but the method can be combined with light scattering and fluorescence flow cytometry.

Discussion and Conclusion

This review gives an overview of (potential) methods for the detection and characterization of microvesicles. Table 1 lists the assessed possibilities and limitations of each method,

based on the underlying physical parameters of each technique.

Considering the optical methods based on light scattering, DLS and NTA are potentially capable of measuring relative and absolute size distributions, respectively, of microvesicles within minutes. Except for Raman spectroscopy, methods based on light scattering cannot distinguish microvesicles from similar-sized lipoprotein particles or small platelets, as no biochemical information is obtained. Raman spectroscopy could potentially detect the size, concentration and biochemical composition of single microvesicles without labeling, but the measurement time is in the order of hours.

Of the optical methods based on fluorescence, STED microscopy, F-NTA and fluorescence correlation spectroscopy are potentially capable of measuring the absolute size distribution and obtaining biochemical information by the application of fluorescent antibody labeling, which is not easy to perform, and involves several practical and optical problems. Real size distribution measurements may be less accurate, as optical detection can be influenced by many factors, such as age of the light source, cleanliness of the cuvette or flow channel, stability of the building and supporting table, and preanalytical conditions.

Among the non-optical methods, TEM and AFM have high (≤ 1 nm) imaging resolution as compared with optical methods. Size and morphology information can be obtained by imaging, and biochemical information can also be obtained. However, measurements are based on many assumptions, and the measurement time is more than 1 h per sample. A fast non-optical method is impedance-based flow cytometry, which can resolve small size differences but only within a limited size range. This technique provides no biochemical information unless combined with fluorescence flow cytometry.

From Table 1, F-NTA seems to be the most suitable method for the detection of size, concentration, biochemical composition and cellular origin of microvesicles at high speed, especially as the method can determine the relevant characteristics of microvesicles directly in body fluids. Nevertheless, the other methods mentioned in this article are being rapidly developed,

and this might lead to new possibilities and shorter measurement times.

Combining methods

Methods that have been successfully combined for microvesicle detection are flow field-flow fractionation (F-FFF) with multiangle light scattering (MALS) or DLS [7]. F-FFF can fractionate 27-nm diameter microvesicles from 36-nm diameter microvesicles [51]. Subsequently, DLS or MALS can accurately determine the size, as the fractionated sample is monodisperse. MALS is based on angle resolved light scattering, and is used for molar mass and mean particle size determination. We did not discuss MALS earlier, because the technique does not provide a size distribution for polydisperse samples. Another method that is practically extendable is Raman spectroscopy, which was recently successfully combined with both Rayleigh scattering and fluorescence microscopy for intracellular chemical analysis [72]. Raman spectroscopy can also be extended with electron microscopy to correlate detailed biochemical information with the relative size distribution and morphology [73]. Finally, Raman spectroscopy can be integrated with optical coherence tomography to obtain quantitative information on the concentration-dependent scattering coefficient [74,75].

Improving methods

A conventional method that can be optimized for the detection of microvesicles is flow cytometry. By reducing flow chamber dimensions, optimizing the flow chamber shape, reducing the flow velocity, and using large-aperture optics, the sensitivity can be increased tremendously. Steen extended a commercial flow cytometer with dark-field illumination and detection to improve the detection limit to 70 nm for polystyrene spheres [42]. Single quantum dots can be detected with 99% accuracy by flow cytometry when a submicrometer fluidic flow channel combined with a confocal microscope is used [76]. NTA is a relatively new method, and is currently showing a high degree of development. Increasing the detector sensitivity and decreasing the wavelength may lower the detection limit to 30 nm for biological particles, so that even the smallest microvesicles come within reach without the need for fluorescent labeling. In specialized laboratories, two impedance-based flow cytometers have been optimized for the detection of submicrometer particles by reducing the channel diameters to 500 and 132 nm [71,77]. In combination with a commercial impedance-based flow cytometer, this covers the whole size range of microvesicles, but centrifugation or filtration of the sample is required to prevent frequent problems with blocking of the flow channel.

Recently obtained results

Recently, some of the methods discussed have been applied to microvesicles [78]. Here, we give an interpretation of these

results based on our analysis. The concentration of microvesicles in platelet-free plasma was reported to be $200\text{--}260 \times 10^9 \text{ L}^{-1}$ by NTA [36] and $3\text{--}702 \times 10^9 \text{ L}^{-1}$ by AFM [5]. It is possible that the real concentration is higher, as the detection efficiency of both methods is $< 100\%$. However, if we consider false positives such as lipoprotein particles, the real concentration may also be lower. With flow cytometry, Yuana obtained a 1000-fold lower CD41⁺-microvesicle concentration, of $11\text{--}291 \times 10^6 \text{ L}^{-1}$, than was obtained with NTA and AFM. The discrepancy in results between flow cytometry and NTA and AFM can be explained by considering the detection limit of commercial flow cytometers, which is insufficient to detect microvesicles smaller than 300 nm. As most microvesicles are smaller than 300 nm and are therefore not detected (Fig. 2A), the detection efficiency is $< 2\%$. In addition, different results have also been obtained with the same method. Lawrie *et al.* [6] used DLS equipment from two companies, and obtained different size distributions for the same microvesicles in fresh frozen plasma. Sources of these differences could be the detection angle and the applied mathematical algorithm.

In conclusion, several (combinations of) methods can correctly detect clinically relevant properties of microparticles and exosomes. These methods should be further explored and validated by comparing measurement results, so that accurate, reliable and fast analyses come within reach.

Acknowledgements

The authors would like to acknowledge J. van Marle and H. A. van Veen (Department of Cell Biology and Histology, University of Amsterdam) for TEM. L.M. van Tiemen, a graduate student of the University of Amsterdam, isolated and imaged microvesicles. We thank M. J. C. van Gemert (Department of Biochemical Engineering and Physics, University of Amsterdam) for useful discussions.

Disclosure of Conflict of Interests

The authors state that they have no conflict of interest.

References

- 1 Simons M, Raposo G. Exosomes – vesicular carriers for intercellular communication. *Curr Opin Cell Biol* 2009; **21**: 575–81.
- 2 Nieuwland R, Sturk A. Why do cells release vesicles? *Thromb Res* 2010; **125**: S49–51.
- 3 Ratajczak J, Wysoczynski M, Hayek F, Janowska-Wieczorek A, Ratajczak MZ. Membrane-derived microvesicles: important and underappreciated mediators of cell-to-cell communication. *Leukemia* 2006; **20**: 1487–95.
- 4 Jy W, Horstman LL, Jimenez JJ, Ahn YS, Biro E, Nieuwland R, Sturk A, Dignat-George F, Sabatier F, Camoin-Jau L, Sampol J, Hugel B, Zobairi F, Freyssinet JM, Nomura S, Shet AS, Key NS, Hebbel RP. Measuring circulating cell-derived microparticles. *J Thromb Haemost* 2004; **2**: 1842–51.
- 5 Yuana Y, Oosterkamp TH, Bahatyrova S, Ashcroft B, Garcia Rodriguez P, Bertina RM, Osanto S. Atomic force microscopy: a novel approach to detect nanosized blood microparticles. *J Thromb Haemost* 2009; **8**: 315–23.

- 6 Lawrie AS, Albanyan A, Cardigan RA, Mackie IJ, Harrison P. Microparticle sizing by dynamic light scattering in fresh-frozen plasma. *Vox Sang* 2009; **96**: 206–12.
- 7 Kang DJ, Oh S, Ahn SM, Lee BH, Moon MH. Proteomic analysis of exosomes from human neural stem cells by flow field-flow fractionation and nanoflow liquid chromatography-tandem mass spectrometry. *J Proteome Res* 2008; **7**: 3475–80.
- 8 Perez-Pujol S, Marker PH, Key NS. Platelet microparticles are heterogeneous and highly dependent on the activation mechanism: studies using a new digital flow cytometer. *Cytometry A* 2007; **71**: 38–45.
- 9 Zwicker JI, Liebman HA, Neuberg D, Lacroix R, Bauer KA, Furie BC, Furie B. Tumor-derived tissue factor-bearing microparticles are associated with venous thromboembolic events in malignancy. *Clin Cancer Res* 2009; **15**: 6830–40.
- 10 Couzin J. Cell biology: the ins and outs of exosomes. *Science* 2005; **308**: 1862–3.
- 11 Burnier L, Fontana P, Kwak BR, Angelillo-Scherrer A. Cell-derived microparticles in haemostasis and vascular medicine. *Thromb Haemost* 2009; **101**: 439–51.
- 12 Conde-Vancells J, Rodriguez-Suarez E, Embade N, Gil D, Matthiesen R, Valle M, Elortza F, Lu SC, Mato JM, Falcon-Perez JM. Characterization and comprehensive proteome profiling of exosomes secreted by hepatocytes. *J Proteome Res* 2008; **7**: 5157–66.
- 13 Thery C, Amigorena S, Raposo G, Clayton A. Isolation and characterization of exosomes from cell culture supernatants and biological fluids. *Curr Protoc Cell Biol* 2006; **Ch 3**: Unit 3.22.
- 14 Thery C, Zitvogel L, Amigorena S. Exosomes: composition, biogenesis and function. *Nat Rev Immunol* 2002; **2**: 569–79.
- 15 Thery C, Ostrowski M, Segura E. Membrane vesicles as conveyors of immune responses. *Nat Rev Immunol* 2009; **9**: 581–93.
- 16 Freysson JM. Cellular microparticles: what are they bad or good for? *J Thromb Haemost* 2003; **1**: 1655–62.
- 17 Cocucci E, Racchetti G, Meldolesi J. Shedding microvesicles: artefacts no more. *Trends Cell Biol* 2009; **19**: 43–51.
- 18 Sims PJ, Faioni EM, Wiedmer T, Shattil SJ. Complement proteins C5b-9 cause release of membrane vesicles from the platelet surface that are enriched in the membrane receptor for coagulation factor Va and express prothrombinase activity. *J Biol Chem* 1988; **263**: 18205–12.
- 19 Nieuwland R, Berckmans RJ, Rotteveel-Eijkman RC, Maquelin KN, Roozendaal KJ, Jansen PG, ten Have K, Eijnsman L, Hack CE, Sturk A. Cell-derived microparticles generated in patients during cardiopulmonary bypass are highly procoagulant. *Circulation* 1997; **96**: 3534–41.
- 20 Giesen PL, Rauch U, Bohrmann B, Kling D, Roque M, Fallon JT, Badimon JJ, Himber J, Riederer MA, Nemerson Y. Blood-borne tissue factor: another view of thrombosis. *Proc Natl Acad Sci USA* 1999; **96**: 2311–15.
- 21 Sims PJ, Wiedmer T, Esmo CT, Weiss HJ, Shattil SJ. Assembly of the platelet prothrombinase complex is linked to vesiculation of the platelet plasma membrane. Studies in Scott syndrome: an isolated defect in platelet procoagulant activity. *J Biol Chem* 1989; **264**: 17049–57.
- 22 Nieuwland R, Berckmans RJ, McGregor S, Boing AN, Romijn FP, Westendorp RG, Hack CE, Sturk A. Cellular origin and procoagulant properties of microparticles in meningococcal sepsis. *Blood* 2000; **95**: 930–5.
- 23 Biro E, Sturk-Maquelin KN, Vogel GM, Meuleman DG, Smit MJ, Hack CE, Sturk A, Nieuwland R. Human cell-derived microparticles promote thrombus formation in vivo in a tissue factor-dependent manner. *J Thromb Haemost* 2003; **1**: 2561–8.
- 24 Valadi H, Ekstrom K, Bossios A, Sjostrand M, Lee JJ, Lotvall JO. Exosome-mediated transfer of mRNAs and microRNAs is a novel mechanism of genetic exchange between cells. *Nat Cell Biol* 2007; **9**: 654–9.
- 25 Deregius MC, Cantaluppi V, Calogero R, Lo Iacono M, Tetta C, Biancone L, Bruno S, Bussolati B, Camussi G. Endothelial progenitor cell derived microvesicles activate an angiogenic program in endothelial cells by a horizontal transfer of mRNA. *Blood* 2007; **110**: 2440–8.
- 26 Al-Nedawi K, Meehan B, Micallef J, Lhotak V, May L, Guha A, Rak J. Intercellular transfer of the oncogenic receptor EGFRvIII by microvesicles derived from tumour cells. *Nat Cell Biol* 2008; **10**: 619–24.
- 27 de Gassart A, Geminard C, Fevrier B, Raposo G, Vidal M. Lipid raft-associated protein sorting in exosomes. *Blood* 2003; **102**: 4336–44.
- 28 Abid Hussein MN, Nieuwland R, Hau CM, Evers LM, Meesters EW, Sturk A. Cell-derived microparticles contain caspase 3 in vitro and in vivo. *J Thromb Haemost* 2005; **3**: 888–96.
- 29 Safaei R, Larson BJ, Cheng TC, Gibson MA, Otani S, Naerdemann W, Howell SB. Abnormal lysosomal trafficking and enhanced exosomal export of cisplatin in drug-resistant human ovarian carcinoma cells. *Mol Cancer Ther* 2005; **4**: 1595–604.
- 30 van Beers EJ, Schaap MC, Berckmans RJ, Nieuwland R, Sturk A, van Doormaal FF, Meijers JC, Biemond BJ. Circulating erythrocyte-derived microparticles are associated with coagulation activation in sickle cell disease. *Haematologica* 2009; **94**: 1513–19.
- 31 Shet AS, Aras O, Gupta K, Hass MJ, Rausch DJ, Saba N, Koopmeiners L, Key NS, Hebbel RP. Sick blood contains tissue factor-positive microparticles derived from endothelial cells and monocytes. *Blood* 2003; **102**: 2678–83.
- 32 Siedlecki CA, Wang IW, Higashi JM, Kottke-Marchant K, Marchant RE. Platelet-derived microparticles on synthetic surfaces observed by atomic force microscopy and fluorescence microscopy. *Biomaterials* 1999; **20**: 1521–9.
- 33 Robert S, Poncellet P, Lacroix R, Arnaud L, Giraud L, Hauchard A, Sampil J, Dignat-George F. Standardization of platelet-derived microparticle counting using calibrated beads and a Cytomics FC500 routine flow cytometer: a first step towards multicenter studies? *J Thromb Haemost* 2009; **7**: 190–7.
- 34 Shah MD, Bergeron AL, Dong JF, Lopez JA. Flow cytometric measurement of microparticles: pitfalls and protocol modifications. *Platelets* 2008; **19**: 365–72.
- 35 Mullier F, Dogné JM, Bailly N, Cornet Y, Robert S, Chatelain B. Accurate quantification of microparticles by flow cytometry: important issues. *J Thromb Haemost* 2009; **7** (Suppl. 2): PP-MO-040.
- 36 Harrison P, Dragovic R, Albanyan A, Lawrie AS, Murphy M, Sargent I. Application of dynamic light scattering to the measurement of microparticles. *J Thromb Haemost* 2009; **7** (Suppl. 2): OC-TU-056.
- 37 van de Hulst HC. *Light Scattering by Small Particles*. New York: Wiley, 1957.
- 38 Bohren CF, Huffman DR. *Absorption and Scattering of Light by Small Particles*. New York, NY: Wiley, 1983.
- 39 van Dijk MA, Lippitz M, Orriit M. Far-field optical microscopy of single metal nanoparticles. *Acc Chem Res* 2005; **38**: 594–601.
- 40 Hoekstra A, Maltsev V, Videen G. *Optics of Biological Particles*. Dordrecht, The Netherlands: Springer, 2007.
- 41 Hoekstra AG, Sloop PMA. Biophysical and biomedical applications of non-spherical scattering. In: Mishchenko MI, Hovenier JW, Travis LD, eds. *Light Scattering by Nonspherical Particles, Theory, Measurements, and Applications*. San Diego, CA: Academic Press, 2000: 585–602.
- 42 Steen HB. Flow cytometer for measurement of the light scattering of viral and other submicroscopic particles. *Cytometry A* 2004; **57**: 94–9.
- 43 Faber DJ, Aalders MCG, Mik EG, Hooper BA, van Gemert MJC, van Leeuwen TG. Oxygen saturation-dependent absorption and scattering of blood. *Phys Rev Lett* 2004; **93**: 28102-1–28102-4.
- 44 Ungureanu C, Rayavarapu RG, Manohar S, van Leeuwen TG. Discrete dipole approximation simulations of gold nanorod optical properties: choice of input parameters and comparison with experiment. *J Appl Phys* 2009; **105**: 102032-1–102032-7.
- 45 de Grooth BG, Terstappen LW, Puppels GJ, Greve J. Light-scattering polarization measurements as a new parameter in flow cytometry. *Cytometry* 1987; **8**: 539–44.

- 46 Clark NA, Lunacek JH, Benedek GB. A study of Brownian motion using light scattering. *Am J Phys* 1970; **38**: 575–85.
- 47 Dieckmann Y, Colfen H, Hofmann H, Petri-Fink A. Particle size distribution measurements of manganese-doped ZnS nanoparticles. *Anal Chem* 2009; **81**: 3889–95.
- 48 Bryant G, Thomas JC. Improved particle-size distribution measurements using multiangle dynamic light-scattering. *Langmuir* 1995; **11**: 2480–5.
- 49 Filella M, Zhang JW, Newman ME, Buffle J. Analytical applications of photon correlation spectroscopy for size distribution measurements of natural colloidal suspensions: capabilities and limitations. *Colloids Surf A Physicochem Eng Asp* 1997; **120**: 27–46.
- 50 Hoo CM, Starostin N, West P, Mecartney ML. A comparison of atomic force microscopy (AFM) and dynamic light scattering (DLS) methods to characterize nanoparticle size distributions. *J Nanopart Res* 2008; **10**: 89–96.
- 51 Korgel BA, van Zanten JH, Monbouquette HG. Vesicle size distributions measured by flow field-flow fractionation coupled with multiangle light scattering. *Biophys J* 1998; **74**: 3264–72.
- 52 Puppels GJ, de Mul FF, Otto C, Greve J, Robert-Nicoud M, Arndt-Jovin DJ, Jovin TM. Studying single living cells and chromosomes by confocal Raman microspectroscopy. *Nature* 1990; **347**: 301–3.
- 53 Uzunbajakava N, Lenferink A, Kraan Y, Volokhina E, Vrensen G, Greve J, Otto C. Nonresonant confocal Raman imaging of DNA and protein distribution in apoptotic cells. *Biophys J* 2003; **84**: 3968–81.
- 54 Puppels GJ, Colier W, Olminkhof JHF, Otto C, Demul FFM, Greve J. Description and performance of a highly sensitive confocal Raman microspectrometer. *J Raman Spectrosc* 1991; **22**: 217–25.
- 55 Pully V, Lenferink A, Otto C. Time-lapse Raman imaging of single live lymphocytes. *J Raman Spectrosc* 2010; doi 10.1002/jrs 2683.
- 56 McCarthy DA. Fluorochromes and fluorescence. In: Macey MG, ed. *Flow Cytometry: Principles and Applications*. New York: Humana Press, 2007: 59–112.
- 57 Zhang Q, Li YL, Tsien RW. The dynamic control of kiss-and-run and vesicular reuse probed with single nanoparticles. *Science* 2009; **323**: 1448–53.
- 58 van Manen HJ, Verkuijlen P, Wittendorp P, Subramaniam V, van den Berg TK, Roos D, Otto C. Refractive index sensing of green fluorescent proteins in living cells using fluorescence lifetime imaging microscopy. *Biophys J* 2008; **94**: L67–9.
- 59 Blum C, Cesa Y, van den Broek JM, Mosk AP, Vos WL, Subramaniam V. Controlling fluorescent proteins by manipulating the local density of photonic states. *Proc SPIE* 2009; **7367**: 73670C-C-9.
- 60 Radbruch A. *Flow Cytometry and Cell Sorting*. New York: Springer, 2000.
- 61 Haugland RP, Spence MTZ, Johnson ID. *The Handbook: A Guide to Fluorescent Probes and Labeling Technologies*. Molecular Probes. Stockton, CA, FatCityBooks, 2005.
- 62 Baumgarth N, Roederer M. A practical approach to multicolor flow cytometry for immunophenotyping. *J Immunol Methods* 2000; **243**: 77–97.
- 63 Westphal V, Hell SW. Nanoscale resolution in the focal plane of an optical microscope. *Phys Rev Lett* 2005; **94**: 143903-1–143903-4.
- 64 Willig KI, Rizzoli SO, Westphal V, Jahn R, Hell SW. STED microscopy reveals that synaptotagmin remains clustered after synaptic vesicle exocytosis. *Nature* 2006; **440**: 935–9.
- 65 Hein B, Willig KI, Hell SW. Stimulated emission depletion (STED) nanoscopy of a fluorescent protein-labeled organelle inside a living cell. *Proc Natl Acad Sci USA* 2008; **105**: 14271–6.
- 66 Ferris MM, Rowlen KL. Detection and enumeration of single nanometric particles: a confocal optical design for fluorescence flow cytometry. *Rev Sci Instrum* 2002; **73**: 2404–10.
- 67 Webb WW. Applications of fluorescence correlation spectroscopy. *Q Rev Biophys* 1976; **9**: 49–68.
- 68 Starchev K, Buffle J, Perez E. Applications of fluorescence correlation spectroscopy: polydispersity measurements. *J Colloid Interf Sci* 1999; **213**: 479–87.
- 69 Pisitkun T, Shen RF, Knepper MA. Identification and proteomic profiling of exosomes in human urine. *Proc Natl Acad Sci USA* 2004; **101**: 13368–73.
- 70 Binnig G, Quate CF, Gerber C. Atomic force microscope. *Phys Rev Lett* 1986; **56**: 930–3.
- 71 Ito T, Sun L, Henriquez RR, Crooks RM. A carbon nanotube-based coulter nanoparticle counter. *Acc Chem Res* 2004; **37**: 937–45.
- 72 Pully VV, Lenferink A, Otto C. Hybrid Rayleigh, Raman and two-photon excited fluorescence spectral confocal microscopy of living cells. *J Raman Spectrosc* 2009; **41**: 599–608.
- 73 van Apeldoorn AA, Aksenov Y, Stigter M, Hofland I, de Bruijn JD, Koerten HK, Otto C, Greve J, van Blitterswijk CA. Parallel high-resolution confocal Raman SEM analysis of inorganic and organic bone matrix constituents. *J R Soc Interface* 2005; **2**: 39–45.
- 74 Faber DJ, van der Meer FJ, Aalders MCG. Quantitative measurement of attenuation coefficients of weakly scattering media using optical coherence tomography. *Opt Express* 2004; **12**: 4353–65.
- 75 Patil CA, Bosschaart N, Keller MD, van Leeuwen TG, Mahadevan-Jansen A. Combined Raman spectroscopy and optical coherence tomography device for tissue characterization. *Opt Lett* 2008; **33**: 1135–7.
- 76 Stavits SM, Edel JB, Samiee KT, Craighead HG. Single molecule studies of quantum dot conjugates in a submicrometer fluidic channel. *Lab Chip* 2005; **88**: 337–43.
- 77 Saleh OA, Sohn LL. Quantitative sensing of nanoscale colloids using a microchip Coulter counter. *Rev Sci Instrum* 2001; **72**: 4449–51.
- 78 Freyssinet JM, Toti F. Membrane microparticle determination: at least seeing what's being sized! *J Thromb Haemost* 2009; **8**: 311–14.